Few-Body Systems 9, 75–87 (1990)

Few-Body Systems

Meson-Nucleon Coupling Constants in a Quark Model*

E. M. Henley, T. Oka**, and J. D. Vergados***

Institute for Nuclear Theory, Department of Physics, FM-15, University of Washington, Seattle, WA 98195, USA

Abstract. An effective vector exchange in a quark model, previously used for nucleon-antinucleon annihilation and meson decays, is applied to nucleon-meson and decuplet baryon-meson couplings. A reasonable fit to experimental data is obtained.

1 Introduction

Mesons are known to be an effective description of nuclear forces at large distances, whereas QCD is expected to be appropriate for very short distances. A variety of models have been used to bridge the gap between these extremes; they include bag models [1], hybrid quark-baryon models [2], and constituent-quark models with confining potentials [3]. In all of these models the pion couples to the quarks or nucleon, and sometimes heavier mesons are also included.

If QCD is the basic theory of strong interactions, it should be possible to calculate the various properties of mesons and nucleons from the theory. However, this is a difficult and presently almost impossible task, except via numerical techniques. For this reason, models have been used to bridge the gap between quarks and hadrons. In previous work we have shown that an effective coloured vector-exchange scheme together with a nonrelativistic constituent-quark model may be used to obtain some hadronic reaction properties. In particular, we have examined the two-meson annihilation of nucleons with antinucleons [4] and the decays of pseudoscalar and vector bosons [5] in this model. Here we apply the model to some allowed baryonic decays and meson-nucleon coupling constants. It should be noted that the pion is treated as a quark-antiquark object, a description which has been found to be reasonable [6]. Neither this assumption nor our model are, of course, unique. Competing models exist [7]. For instance, it has also been proposed that

* This article is written in honour and memory of Michael Moravcsik. He was both a dedicated physicist and a very humane person with wide interests in the world around him. One of us (EMH) knew him well and will continue to cherish his friendship

** Kure Women's Junior College, Kure, Hiroshima-ken 737, Japan

*** Theoretical Physics Division, University of Ioannina, GR-45332 Ioannina, Greece

the pion is a Goldstone boson, a collective state, or may have properties of combinations of these models [8]. However, we develop the effective coloured vector-exchange model in order to determine its successes and inadequacies.

It should be noted that our model is a nonrelativistic one. This approximation continues to be useful in nucleon structure calculations [3] but can certainly be questioned, since the quark mass and its momentum are both about the same order of magnitude. Nevertheless, we expect that the nonrelativistic approach gives a result that is accurate to about 25%, which is not so different from the accuracy of other approaches. For instance, the meson-nucleon coupling constants have been calculated in a chiral soliton model [9]; this approach is valid to leading order in $1/N_c$, where N_c is the number of colours, and therefore to about 30%. Recently, a number of relativistic approaches have been proposed for mesons, but we have not implemented them here; they are much more complex and make it more difficult to get deeper physical insights [10].

2 Theory

In our model, the basic diagram responsible for the baryon-baryon-meson coupling is $q \to qq\bar{q}$ as shown in Fig. 1. We use a nonrelativistic reduction of the matrix element associated with Fig. 1. The matrix element up to first order of momenta is given by [4, 5]

$$v_{ij}(\vec{q}, \vec{p}_i) = -g_s^2 \frac{\vec{\lambda}_i \cdot \vec{\lambda}_j}{4} \frac{1}{\omega_q^2 - q^2} \left[\frac{\vec{\sigma}_j \cdot \vec{q}}{2} \left(\frac{1}{m_i} + \frac{1}{m_j} \right) - \frac{i\vec{\sigma}_i \times \vec{\sigma}_j \cdot \vec{q}}{2m_i} - \frac{\vec{\sigma}_j \cdot \vec{p}_i}{m_i} \right], \quad (1)$$

where $\vec{q} = \vec{p}_i - \vec{p}\,'_i$, $\omega_q = E_{p_i} - E_{p'_i}$, $\sigma_i(m_i)$ is the spin (constituent mass) of quark i, g_s is the strong coupling constant and $\vec{\lambda}_i \cdot \vec{\lambda}_j/4$ is the colour factor.

For the vector propagator, which can be thought of as one, or more, correlated gluons, we consider two extreme cases: (Case A) we neglect the energy transferred by the vector, i.e. $\omega_q \simeq 0$, and (Case B) we neglect the three-momentum, $\vec{q}$, transferred by the vector and make the approximation $\omega_q = \text{constant} \simeq 2m_j$. For the quark wave functions of low-lying baryons and mesons we use the $SU(6)$ basis with ground states of orbital angular momentum = 0, i.e., S-states. The baryon and meson wave functions with momenta $\vec{P}$ and $\vec{q}$, respectively, are

$$\psi_B(\vec{P}) = \frac{\exp[i\vec{P} \cdot \vec{R}]}{3^{3/4}} \psi_{0,B} \psi_{SI,B} \psi_{C,B}, \quad (2a)$$

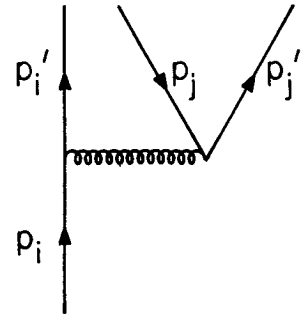

Fig. 1. The basic diagram responsible for the baryon-baryon-meson interaction in the effective coloured vector-particle exchange approximation

and

$$\psi_M(\vec{q}) = \frac{\exp[i\vec{q}\cdot\vec{R}']}{2^{3/4}}\psi_{0,M}\psi_{SI,M}\psi_{C,M}, \tag{3a}$$

where $\vec{R}$ ($\vec{R}'$) is the c.m. coordinate of the baryon (meson), and $\psi_{SI,B}$ ($\psi_{SI,M}$) and $\psi_{C,B}$ ($\psi_{C,M}$) are the spin-isospin (flavour) and colour wave functions of the baryon (meson), respectively. The baryon and meson spatial wave functions $\psi_{0,B}$ and $\psi_{0,M}$ are

$$\psi_{0,B}(\vec{\xi},\vec{\eta}) = \frac{\exp\left[-\frac{\xi^2+\eta^2}{2b^2}\right]}{(\sqrt{\pi}\,b)^3} \tag{2b}$$

and

$$\psi_{0,M}(\vec{\xi}_1) = \frac{\exp\left[-\frac{\xi_1^2}{2b_m^2}\right]}{(\sqrt{\pi}\,b_m)^{3/2}}, \tag{3b}$$

where b and b_m are the harmonic-oscillator parameters for the baryon and meson, respectively. Here $\vec{\xi}$, $\vec{\eta}$, and $\vec{\xi}_1$ are the relative coordinates; see also Eq. (4).

We evaluate the baryon-baryon-meson interaction matrix element for the case shown in Fig. 2. Basically there are two types of diagrams, Fig. 2a, the "direct" diagram, and Fig. 2b, the "exchange" diagram.

The calculation of the matrix element is straightforward, and separates into space, spin-isospin, and colour matrix elements. The spatial matrix element takes the form

$$\begin{aligned}\mathcal{R} = \frac{1}{2^{3/4}3^{3/2}}\int d\vec{x}_1\, d\vec{x}_2\, d\vec{x}_3\, d\vec{x}_4 \\ \times \exp\left[i\frac{\vec{P}\cdot(\vec{x}_1+\vec{x}_2+\vec{x}_3)}{3}\right]\exp\left[-i\frac{\vec{P}_1\cdot(\vec{x}_1+\vec{x}_2+\vec{x}_4)}{3}\right] \\ \times \exp\left[-i\frac{\vec{P}_2(\vec{x}_3+\vec{x}_4)}{2}\right]\psi^*_{0,B}\left(\frac{\vec{x}_1-\vec{x}_2}{\sqrt{2}},\frac{\vec{x}_1+\vec{x}_2-2\vec{x}_4}{\sqrt{6}}\right)\psi^*_{0,M}\left(\frac{\vec{x}_3-\vec{x}_4}{\sqrt{2}}\right) \\ \times v(\vec{r}=\vec{x}_i-\vec{x}_4,\vec{x}_i)\psi_{0,B}\left(\frac{\vec{x}_1-\vec{x}_2}{\sqrt{2}},\frac{\vec{x}_1+\vec{x}_2-2\vec{x}_3}{\sqrt{6}}\right),\end{aligned} \tag{4}$$

where $\vec{P}$, $\vec{P}_1$, and $\vec{P}_2$ are the three momenta of the initial baryon, final baryon and meson, respectively (see Fig. 2). In Eq. (4) the interaction $v(\vec{r}=\vec{x}_i-\vec{x}_4,\vec{x}_i)$ is

$$v^{\mathrm{A}}(\vec{r}=\vec{x}_i-\vec{x}_4,\vec{x}_i) = -i\alpha_s\frac{\vec{\lambda}_i\cdot\vec{\lambda}_4}{4}\frac{1}{2r}\left[\left(\frac{\vec{\sigma}_4}{m_i}+\frac{\vec{\sigma}_4}{m_4}-i\frac{\vec{\sigma}_i\times\vec{\sigma}_4}{m_i}\right)\cdot\frac{\vec{r}}{r^2}-\frac{2\vec{\sigma}_4\cdot\vec{\nabla}_{x_i}}{m_i}\right], \tag{5a}$$

$$\begin{aligned}v^{\mathrm{B}}(\vec{r}=\vec{x}_i-\vec{x}_4,\vec{x}_i) = i\frac{\alpha_s\pi}{2m_4^2}\frac{\vec{\lambda}_i\cdot\vec{\lambda}_4}{4}\delta(\vec{r})\left[\left(\frac{\vec{\sigma}_4}{m_i}+\frac{\vec{\sigma}_4}{m_4}-\frac{i\vec{\sigma}_i\times\vec{\sigma}_4}{m_i}\right)\right. \\ \left.\cdot(\overleftarrow{\nabla}_{x_i}+\vec{\nabla}_{x_i})-\frac{2\vec{\sigma}_4\cdot\vec{\nabla}_{x_i}}{m_i}\right],\end{aligned} \tag{5b}$$

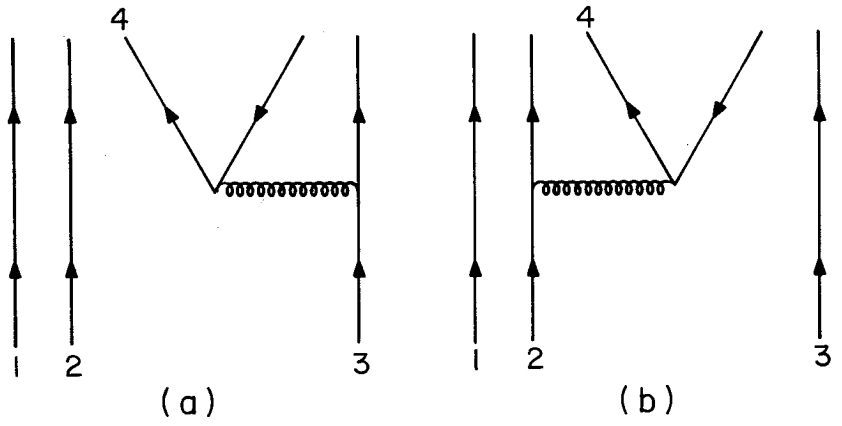

Fig. 2. The baryon-baryon-meson interaction; **a** is the "direct" diagram and **b** is the "exchange" one

for cases A and B, respectively, where $i = 3$ and 2 for Figs. 2a and b, respectively, $\alpha_s = g_s^2/4\pi$ and $\vec{\nabla}_{x_i}$ ($\overleftarrow{\nabla}_{x_i}$) acts on the initial- (final-) state wave function. The first parenthesis in Eqs. (5) is the local contribution whereas the last term is the momentum-dependent or nonlocal one. In the plane-wave terms of Eq. (4) we neglect the quark mass difference for simplicity. This neglect is justified for the case of up and down quarks and accurate to about 10% with the inclusion of a strange quark.

Performing integrations in Eq. (4), we obtain

$$\mathscr{R} = (2\pi)^3 \delta(\vec{P} - \vec{P}_1 - \vec{P}_2)\mathscr{M}, \tag{6}$$

$$\mathscr{M}_{\text{dir}} = \alpha_s \frac{\vec{\lambda}_3 \cdot \vec{\lambda}_4}{4} Y_d \left[\vec{A}_d \cdot \vec{q}\, X_{1,d} + \vec{A}_d \cdot \vec{Q}\, X_{2,d} + \frac{\vec{\sigma}_4 \cdot \vec{q}}{m_3} X_{3,d} + \frac{\vec{\sigma}_4 \cdot \vec{Q}}{m_3} X_{4,d} \right], \tag{7a}$$

and

$$\mathscr{M}_{\text{exch}} = \alpha_s \frac{\vec{\lambda}_2 \cdot \vec{\lambda}_4}{4} Y_e \left[\vec{A}_e \cdot \vec{q}\, X_{1,e} + \vec{A}_e \cdot \vec{Q}\, X_{2,e} + \frac{\vec{\sigma}_4 \cdot \vec{q}}{m_2} X_{3,e} + \frac{\vec{\sigma}_4 \cdot \vec{Q}}{m_2} X_{4,e} \right], \tag{7b}$$

where $\vec{q} = \vec{P} - \vec{P}_1 = \vec{P}_2$ and $\vec{Q} = \vec{P} + \vec{P}_1$. In Eqs. (7), the terms from the local interaction are $\vec{A}_d$ and $\vec{A}_e$, with

$$\vec{A}_d = \frac{\vec{\sigma}_4}{m_3} + \frac{\vec{\sigma}_4}{m_4} - i\frac{\vec{\sigma}_3 \times \vec{\sigma}_4}{m_3}, \tag{8a}$$

and

$$\vec{A}_e = \frac{\vec{\sigma}_4}{m_2} + \frac{\vec{\sigma}_4}{m_4} - i\frac{\vec{\sigma}_3 \times \vec{\sigma}_4}{m_2}. \tag{8b}$$

The results for Y_d, $X_{1,d}$ to $X_{4,d}$ and Y_e, $X_{1,e}$ to $X_{4,e}$ are given in Appendix A.

The colour factor is (see Fig. 2)

$$\left\langle \frac{\vec{\lambda}_3 \cdot \vec{\lambda}_4}{4} \right\rangle = \frac{4}{3\sqrt{3}}, \tag{9a}$$

for the direct diagram, and

$$\left\langle \frac{\vec{\lambda}_2 \cdot \vec{\lambda}_4}{4} \right\rangle = -\frac{2}{3\sqrt{3}}, \tag{9b}$$

Table 1. The spin-isospin factor for $NN\pi$ and $NN\eta$ interactions for direct and exchange diagrams

		A	A'
$NN\pi$	Direct	$-5/6$	$5/3$
	Exchange	$-5/3$	0
$NN\eta$	Direct	$-1/2\sqrt{3}$	$1/\sqrt{3}$
	Exchange	$-1/\sqrt{3}$	0

Table 2. The spin-isospin factor for $NN\rho$ and $NN\omega$ interactions for direct and exchange diagrams

		B	C	B'	C'
$NN\rho$	Direct	$-\frac{1}{2}$	$\frac{5}{6}$	-1	0
	Exchange	-1	$\frac{5}{3}$	$-\frac{2}{3}$	$-\frac{1}{3}$
$NN\omega$	Direct	$-\frac{3}{2}$	$\frac{1}{2}$	-3	0
	Exchange	-3	1	2	1

for the exchange diagram. The spin-isospin factor is found to be

$$\langle\psi_{S-I}|\vec{\sigma}_4\cdot\vec{k}|\psi_{S-I}\rangle = A\vec{\sigma}_N\cdot\vec{k}, \tag{10a}$$

$$\langle\psi_{S-I}|-i\vec{\sigma}_i\times\vec{\sigma}_4\cdot\vec{k}|\psi_{S-I}\rangle = A'\vec{\sigma}_N\cdot\vec{k}, \tag{10b}$$

for the nucleon-pseudoscalar-meson interaction, and

$$\langle\psi_{S-I}|\vec{\sigma}_4\cdot\vec{k}|\psi_{S-I}\rangle = B\vec{k}\cdot\vec{\varepsilon} + C(-i\vec{\sigma}_N\times\vec{k})\cdot\vec{\varepsilon}, \tag{10c}$$

$$\langle\psi_{S-I}|(-i\vec{\sigma}_i\times\vec{\sigma}_4)\cdot\vec{k}|\psi_{S-I}\rangle = B'\vec{k}\cdot\vec{\varepsilon} + C'(-i\vec{\sigma}_N\times\vec{k})\cdot\vec{\varepsilon}, \tag{10d}$$

for the nucleon-vector-meson interaction. Here $\vec{k}$ is an arbitrary three-momentum vector $\vec{\sigma}_N$ and $\vec{\varepsilon}$ are the spin operator for the nucleon and the polarization of the vector meson, respectively. The values for A and A' are listed in Table 1 for the nucleon-pion ($NN\pi$) and nucleon-eta ($NN\eta$) cases. Table 2 shows the values of B, B', C, and C' for the nucleon-rho ($NN\rho$) and nucleon-omega ($NN\omega$) interactions. The isospin wave function of the ω used here is $\omega = (u\bar{u} + d\bar{d})/\sqrt{2}$, since the ϕ-meson is pure (or almost pure) $s\bar{s}$. The η and η', on the other hand are almost pure octet and singlet, so that the isospin-zero combination is $(u\bar{u} + d\bar{d})/\sqrt{2} = \eta/\sqrt{3} + \sqrt{2}\eta'/\sqrt{3}$. Because the s quark does not contribute, the effective part of η is "η" $\equiv (u\bar{u} + d\bar{d})/\sqrt{6}$.

3 Results

With the results of the spatial integrals from Eq. (7), the colour factors of Eq. (9), and the spin-isospin matrices of Eq. (10), one obtains the following $NN\pi$ and $NN\eta$ interactions in an arbitrary frame of reference,

$$\mathscr{L}_{NN\pi} = -\alpha_s \frac{10}{9\sqrt{3}} \frac{\sqrt{2E_\pi}}{m} [\vec{\sigma}_N \cdot \vec{q}\{Y_d X_{3,d} - Y_e(2X_{1,e} + X_{3,e})\} + \vec{\sigma}_N \cdot \vec{Q}\{Y_d X_{4,d} - Y_e(2X_{2,e} + X_{4,e})\}] \vec{\tau} \cdot \vec{\phi}, \tag{11a}$$

$$\mathscr{L}_{NN\eta} = -\alpha_s \frac{2}{9} \frac{\sqrt{2E_\eta}}{m} [\vec{\sigma}_N \cdot \vec{q}\{Y_d X_{3,d} - Y_e(2X_{1,e} + X_{3,e})\} + \vec{\sigma}_N \cdot \vec{Q}\{Y_d X_{4,d} - Y_e(2X_{2,e} + X_{4,e})\}], \tag{11b}$$

where m is the quark mass of the up and down quarks and E_π, E_η are the energies of the pion and eta meson. We take $m = 330$ MeV and $E_\pi \approx m_\pi$, $E_\eta = m_\eta$ for comparison with experimental data.

The interactions are given by

$$\mathscr{L}_{NN\pi} = i g_{NN\pi} \bar{\psi} \gamma_5 \vec{\tau} \psi \vec{\phi} \simeq \frac{i g_{NN\pi}}{2M} \vec{\sigma}_N \cdot \vec{q}\, \vec{\tau} \cdot \vec{\phi}, \tag{12a}$$

and

$$\mathscr{L}_{NN\eta} = i g_{NN\eta} \bar{\psi} \gamma_5 \psi \phi \simeq \frac{i g_{NN\eta}}{2M} \vec{\sigma}_N \cdot \vec{q}, \tag{12b}$$

where M is the nucleon mass.

We use the leading nonrelativistic (static) approximation to get the approximate second equality in Eqs. (12). The experimental value of $|g_{NN\pi}|/(2M)$ is

$$\frac{|g_{NN\pi}|}{2M} = 7.14 \times 10^{-3}\ \text{MeV}^{-1}, \tag{13}$$

which is obtained from $|g_{NN\pi}|^2/(4\pi) = 14.3$ (ref. [11]).

Table 3. The values of α_s required to fit the $NN\pi$ vertex for cases A and B. Also shown are the ratios of the $(\vec{\sigma}_N \cdot \vec{Q})$-contribution to that of $\vec{\sigma}_N \cdot \vec{q}$, of the exchange diagram to the direct one in $\vec{\sigma}_N \cdot \vec{q}$, and of the nonlocal term to the local one in $\vec{\sigma}_N \cdot \vec{q}$ for cases A and B, where higher powers of Q and q are neglected

b (fm)		0.4	0.6	0.6	0.8	0.8	0.8
b_m (fm)		0.4	0.4	0.6	0.4	0.6	0.8
Case A	α_s	2.3	1.8	1.8	1.7	1.5	1.6
	$\frac{\langle \vec{\sigma}_N \cdot \vec{Q} \rangle}{\langle \vec{\sigma}_N \cdot \vec{q} \rangle}$	−0.096	0.011	−0.096	0.079	−0.019	−0.096
	$\frac{\text{Exchange contribution}}{\text{Direct contribution}}$	0.15	0.12	0.15	0.10	0.13	0.15
	$\frac{\text{Nonlocal contribution}}{\text{Local contribution}}$	3.7	4.1	3.7	4.9	4.0	3.7
Case B	α_s	3.9	4.5	7.3	4.9	7.9	11
	$\frac{\langle \vec{\sigma}_N \cdot \vec{Q} \rangle}{\langle \vec{\sigma}_N \cdot \vec{q} \rangle}$	0.043	0.15	0.043	0.22	0.12	0.043
	$\frac{\text{Exchange contribution}}{\text{Direct contribution}}$	0.41	0.24	0.41	0.14	0.29	0.41
	$\frac{\text{Nonlocal contribution}}{\text{Local contribution}}$	1.1	2.0	1.1	3.8	1.6	1.1

In Table 3 the values of α_s consistent with experiment, Eq. (13), are listed for various sizes of b and b_m. In the comparison of Eq. (11 a) with Eq. (12 a) we use only the term proportional to $\vec{\sigma}\cdot\vec{q}$. The ratios of the coefficients of the $\vec{\sigma}_N\cdot\vec{Q}$ to the $\vec{\sigma}_N\cdot\vec{q}$ terms, of the exchange diagram to the direct one in the $\vec{\sigma}_N\cdot\vec{q}$ term, and of the nonlocal term to the local one in the $\vec{\sigma}_N\cdot\vec{q}$ term, are also shown in Table 3.

The experimental ratio of $|g_{NN\eta}/g_{NN\pi}|$ is [11]

$$\left|\frac{g_{NN\eta}}{g_{NN\pi}}\right| \approx 0.55, \tag{14}$$

with an error of about 20%, and is obtained from $|g_{NN\eta}|^2/(4\pi) \approx 4.3$ (ref. [11]). In our calculation we obtain for the ratio

$$\left|\frac{g_{NN\eta}}{g_{NN\pi}}\right| = \frac{\sqrt{3m_\eta}}{5\sqrt{m_\pi}} \simeq 0.69, \tag{15}$$

independent of the choice of b and b_m.

The $NN\rho$ and $NN\omega$ interactions are also obtained and can be expressed as

$$\mathscr{L}_{NN\rho} = F_1^\rho[\vec{Q} + (1+F_2^\rho)(-i\vec{\sigma}_N\times\vec{q}) + R_1^\rho\vec{q} + R_2^\rho(-i\vec{\sigma}_N\times\vec{Q})]\tau_\alpha\cdot\vec{\rho}_\alpha, \tag{16 a}$$

$$\mathscr{L}_{NN\omega} = F_1^\omega[\vec{Q} + (1+F_2^\omega)(-i\vec{\sigma}_N\times\vec{q}) + R_1^\omega\vec{q} + R_2^\omega(-i\vec{\sigma}_N\times\vec{Q})\cdot\vec{\omega}. \tag{16 b}$$

The effective $NN\rho$ and $NN\omega$ interactions are given by

$$\mathscr{L}_{NN\rho} = g_{NN\rho}\bar{\psi}\left[\gamma_\mu + \frac{\mu_\rho}{2M}i\sigma_{\mu\nu}(p'-p)^\nu\right]\tau_\alpha\psi\rho_\alpha^\mu$$

$$\simeq -\frac{g_{NN\rho}}{2M}\{\vec{Q} + (1+\mu_\rho)(-i\vec{\sigma}_N\times\vec{q})\}\tau_\alpha\cdot\vec{\rho}_\alpha, \tag{17 a}$$

$$\mathscr{L}_{NN\omega} = g_{NN\omega}\bar{\psi}\left[\gamma_\mu + \frac{\mu_\omega}{2M}i\sigma_{\mu\nu}(p'-p)^\mu\right]\psi\omega^\mu$$

$$\simeq -\frac{g_{NN\omega}}{2M}\{\vec{Q} + (1+\mu_\omega)(-i\vec{\sigma}_N\times\vec{q})\}\cdot\vec{\omega}, \tag{17 b}$$

where we use the nonrelativistic approximation of the space components to get the second equality on the right-hand side. The experimental values of $g_{NN\rho}/2M$ and μ_ρ are [11]

$$\frac{|g_{NN\rho}|}{2M} = (1.4\pm0.1)\times10^{-3}\ \mathrm{MeV}^{-1}, \tag{18 a}$$

$$\mu_\rho \simeq 6.1\pm0.6, \tag{18 b}$$

where $|g_{NN\rho}|^2/(4\pi) = 0.55\pm0.06$ is used. The experimental values of $g_{NN\omega}$ and μ_ω are not known as well [11],

$$\frac{|g_{NN\omega}|}{2M} = (4.6\pm2.3)\times10^{-3}\ \mathrm{MeV}^{-1}, \tag{19 a}$$

$$\mu_\omega = -0.3 \text{ to } 1.1, \tag{19 b}$$

where $|g_{NN\omega}|^2/(4\pi) = 6\pm3$ is used.

The values of α_s which fit the central value of Eqs. (18 a) and (19 a) are shown in Tables 4 and 5, respectively; so are F_2, R_1, R_2, the ratio of exchange to direct diagram in F_1 and F_2, and the ratio of the nonlocal term to the local one.

The coupling constants for the pion to the decuplet ($S = \frac{3}{2}$) and octet ($S = \frac{1}{2}$) are directly related to the decay rates. Next, we thus examine the pionic decays of $J^P = \frac{3}{2}^+$ baryons: $\Delta^{++} \to P\pi^+$, $\Sigma^{*+} \to \Sigma\pi$, and $\Xi^{*0} \to \Xi\pi$. In the rest frame of the initial baryon, the matrix elements for these decays can be written as

$$\mathcal{M}_{\text{dir}} = \frac{\vec{\lambda}_3 \cdot \vec{\lambda}_4}{4} Y_d \frac{q_+}{m} C_g [X_{3,d} - X_{4,d}], \tag{20 a}$$

$$\mathcal{M}_{\text{exch}} = \frac{\vec{\lambda}_2 \cdot \vec{\lambda}_4}{4} Y_e \frac{q_+}{m} C_g [a_1(X_{1,e} - X_{2,e}) + a_2(X_{3,e} - X_{4,e})], \tag{20 b}$$

for the direct and exchange diagrams, respectively, with $\vec{\lambda}_2 \cdot \vec{\lambda}_4 \approx -\frac{1}{2}\vec{\lambda}_3 \cdot \vec{\lambda}_4$. The matrix element in Eqs. (20) is given for the decay of an $S = S_z = \frac{3}{2}$ state to an $S = S_z = \frac{1}{2}$ baryon and a meson of momentum q with component $q_+ = -(q_x + iq_y)/\sqrt{2}$.

The coefficients C_g, a_1, and a_2 are given in Table 6. The decay rate in the rest frame of the decaying particle is given by

Table 4 a. The values of α_s, F_2^ρ, R_1^ρ, and R_2^ρ for the $NN\rho$ vertex are given for case A. The ratios of the contributions from the exchange diagram to the direct one and nonlocal term to the local one are also listed

b (fm)		0.4	0.6	0.6	0.8	0.8	0.8
b_m (fm)		0.4	0.4	0.6	0.4	0.6	0.8
α_s		1.1	1.4	0.92	1.9	1.0	0.80
F_2^ρ		4.9	8.1	4.9	13	6.9	4.9
R_1^ρ		−3.9	−5.9	−3.9	−8.9	−5.2	−3.9
R_2^ρ		−1.2	−0.84	−1.2	−0.33	−0.97	−1.1
Exchange	In term $\propto \vec{Q}$	−15	−4.3	−15	−2.7	−5.6	−15
Direct	In term $\propto -i\vec{\sigma} \times \vec{q}$	0.12	0.10	0.12	0.082	0.11	0.12
Nonlocal	In term $\propto \vec{Q}$	1.0	0.067	1.0	−0.36	0.29	1.0
Local	In term $\propto -i\vec{\sigma} \times \vec{q}$	4.1	4.6	4.1	5.4	4.4	4.1

Table 4 b. Same as for Table 4 a, but for case B

b (fm)		0.4	0.6	0.6	0.8	0.8	0.8
b_m (fm)		0.4	0.4	0.6	0.4	0.6	0.8
α_s		1.4	1.7	2.5	1.9	2.9	3.9
F_2^ρ		3.0	3.3	3.0	3.6	3.2	3.0
R_1^ρ		−2.9	−3.0	−2.9	−3.0	−3.0	−2.9
R_2^ρ		−0.85	−0.53	−0.85	−0.33	−0.62	−0.85
Exchange	In term $\propto \vec{Q}$	0.68	0.38	0.68	0.22	0.46	0.68
Direct	In term $\propto -i\vec{\sigma} \times \vec{q}$	0.34	0.20	0.34	0.11	0.24	0.34
Nonlocal	In term $\propto \vec{Q}$	0.16	−0.24	0.16	−0.37	−0.16	0.16
Local	In term $\propto -i\vec{\sigma} \times \vec{q}$	1.2	2.3	1.2	4.2	1.8	1.2

Table 5a. Same as Table 4a, but for $NN\omega$ coupling; case A

b (fm)		0.4	0.6	0.6	0.8	0.8	0.8
b_m (fm)		0.4	0.4	0.6	0.4	0.6	0.8
α_s		1.1	1.4	0.91	1.9	1.0	0.79
F_2^ω		0.21	0.88	0.21	1.8	0.63	0.21
R_1^ω		−3.1	−4.8	−3.1	−7.4	−4.1	−3.1
R_2^ω		−0.19	−0.13	−0.19	−0.043	−0.15	−0.19
Exchange	In term $\propto \vec{Q}$	−17	−4.6	−17	−2.8	−6.0	−17
Direct	In term $\propto -i\vec{\sigma} \times \vec{q}$	0.27	0.23	0.27	0.19	0.24	0.27
Nonlocal	In term $\propto \vec{Q}$	0.84	0.062	0.84	−0.34	0.26	0.84
Local	In term $\propto -i\vec{\sigma} \times \vec{q}$	2.4	2.8	2.4	3.2	2.6	2.4

Table 5b. Same as Table 4b, but for $NN\omega$; case B

b (fm)		0.4	0.6	0.6	0.8	0.8	0.8
b_m (fm)		0.4	0.4	0.6	0.4	0.6	0.8
α_s		1.3	1.7	2.4	2.0	2.9	3.6
F_2^ω		−0.10	−0.017	−0.10	0.0064	−0.035	−0.10
R_1^ω		−1.8	−2.3	−1.8	−2.5	−2.1	−1.8
R_2^ω		−0.10	−0.082	−0.10	−0.056	−0.091	−0.10
Exchange	In term $\propto \vec{Q}$	0.96	0.47	0.96	0.25	0.59	0.96
Direct	In term $\propto -i\vec{\sigma} \times \vec{q}$	0.75	0.45	0.75	0.26	0.54	0.75
Nonlocal	In term $\propto \vec{Q}$	0.13	−0.23	0.13	−0.37	−0.15	0.13
Local	In term $\propto -i\vec{\sigma} \times \vec{q}$	0.71	1.4	0.71	2.5	1.1	0.71

Table 6. Coefficients C_g, a_1, and a_2 for $(J^P = \frac{3}{2}^+)$-baryon pionic decays: $\Delta^{++} \to N\pi$, $\Sigma^{*+} \to \Sigma\pi$ and $\Lambda\pi$, and $\Xi^{*0} \to \Xi\pi$. The experimental partial widths are also shown. The parameter r denotes $r \equiv m/m_s$

	Experimental partial width [17] (MeV)	C_g	a_1	a_2
$\Delta^{++}(1232) \to N\pi$	114 ± 5	$-\sqrt{2}$	1	2
$\Sigma^{*+}(1385) \to \Sigma\pi$	4.3 ± 0.8	$\sqrt{\frac{2}{3}}$	$\frac{4}{3} - \frac{r}{3}$	$1 + r$
$\Sigma^{*+}(1385) \to \Lambda\pi$	32 ± 2	−1	$\frac{4}{3} - \frac{r}{3}$	$1 + r$
$\Xi^{*0}(1530) \to \Xi\pi$	9.1 ± 0.5	1	$2 - r$	$2r$

$$\Gamma = \frac{|\mathcal{M}_{\text{dir}} + \mathcal{M}_{\text{exch}}|^2}{3} \frac{qE_N}{2\pi M} \cdot 2E_\pi, \tag{21}$$

where q, E_N, and M are the momentum of the pion, the energy of the baryon, and the mass of the decaying particle, respectively. The factor of 3 arises because

Table 7. Table of a_s for the pionic decays of Δ^{++}, Σ^{*+}, and Ξ^{*0}. The central values of the experimental partial widths are used

b (fm)		0.4	0.6	0.6	0.8	0.8	0.8
b_m (fm)		0.4	0.4	0.6	0.4	0.6	0.8
Case A	$\Delta^{++} \to N\pi$	2.2	2.0	1.9	2.1	1.8	1.7
	$\Sigma^{*+} \to \Sigma\pi$	2.2	2.0	1.9	2.0	1.7	1.6
	$\Sigma^{*+} \to \Lambda\pi$	2.0	1.8	1.7	1.9	1.6	1.5
	$\Xi^{*0} \to \Xi\pi$	1.8	1.6	1.5	1.6	1.4	1.4
Case B	$\Delta^{++} \to N\pi$	5.5	7.0	11	8.1	13	17
	$\Sigma^{*+} \to \Sigma\pi$	5.5	6.6	10	7.2	12	16
	$\Sigma^{*+} \to \Lambda\pi$	4.9	6.0	9.3	6.9	11	15
	$\Xi^{*0} \to \Xi\pi$	4.2	5.0	7.9	5.6	9.1	12

$\langle |q_+|^2 \rangle = q^2/3$. The values of α_s extracted from the central values of the decay widths are listed in Table 7.

4 Discussion

There are a number of general observations to be made about the results presented in Tables 3 to 5.

We believe that case A may be closer to the truth than case B. In the nucleon-nucleon force or other potential models, which involve meson exchanges, the meson carries only three-momentum but no energy. Thus, the three-momentum of the exchanged vector is likely to be more important than the energy, and this corresponds to model A.

The values of α_s obtained for scheme A are relatively independent of the radii chosen for the nucleon and meson. They are somewhat more dependent on the choice of radii for case B. The values obtained are quite reasonable and compare favourably to those obtained in $N\bar{N}$ annihilation and meson decays [4, 5]. The values of α_s for the ω and ρ are smaller by about a factor 2 than those for the π and η except for $b = 0.8$ fm, $b_m = 0.4$ fm and $b = 0.6$ fm, $b_m = 0.4$ fm, when they are almost equal. We cannot easily account for the large variation of α_s in going from pseudoscalar to vector mesons for other cases of b and b_m.

The values of α_s found for the pionic decays of the decuplet, e.g. Δ, are very similar to those deduced for the $NN\pi$ coupling constant. They show only a small dependence on radii and are almost independent of the decaying particle. The slight variation of α_s with the mass of the decaying particle is approximately what might be expected from the momentum dependence of α_s (ref. [4]). The value of α_s is insensitive to the mass of the s-quark. The values are almost identical for $m_s = 510$ and 580 MeV.

The meson-nucleon couplings include recoil corrections. For instance, the pion-nucleon interaction not only has a local nucleon term, proportional to $\vec{q}$, but also a nonlocal term proportional to $\vec{Q}$. The latter is a recoil term and is of the order of magnitude and sign expected for a Galilean invariant pion-nucleon coupling [12].

In this case, the interaction, Eqs. (11), should only depend on the relative velocity between the pion and nucleon in the nonrelativistic limit or it should be proportional to[1]

$$\mathscr{L}_{NN\pi} \propto \sigma_N \cdot \left(\vec{q} - \frac{m_\pi}{2M} \vec{Q} \right). \tag{22}$$

Since the ratio $m_\pi/2M$ is of the order of 1/14 it is quite small, as found in our work. The correction for the η-meson is the same, so that it is the average pseudoscalar-meson mass which should appear in Eq. (22). In the case of the vector mesons, the ratio of term proportional to $\vec{q}$ relative to that proportional to $\vec{Q}$ should be $-2M/m_\rho \approx -2.4$. Both the order of magnitude and sign of R are approximately correct. The same holds for R_2, which should be $\approx -1/2.4$, as observed from Tables 4 and 5. Both the sign and magnitude agree with the result outlined in Tables 5 and 6 for the vector mesons. For the pion the magnitude is correct, but the sign varies with radius. This change comes from other recoil corrections included in our model.

It is well known that there is no unique definition of a meson-nucleon coupling constant. Thus, it is not surprising that the magnitude of the coupling constants we obtain depend on the frame of reference. For instance, the nonrelativistic approximation for the nucleons is satisfied most closely in the Breit frame, where both the initial and final nucleon have momenta equal in magnitude to half that of the meson, $|\vec{q}/2|$. In this frame the value of $\vec{Q}$ vanishes. On the other hand, for an initial baryon at rest, the magnitudes of $\vec{Q}$ and $\vec{q}$ are equal to each other. We have chosen an arbitrary frame of reference by keeping recoil terms, but make the comparison with experimentally determined coupling constants by means of the "leading" terms, alone.

The ratios of the exchange to direct-diagram contributions shown in the various tables are primarily useful as an aid to the reader. On the other hand, the ratio of the nonlocal to local term is shown because some authors neglect the velocity-dependent term in the basic process [13], Fig. 1 and Eq. (1). In general, the contribution of the velocity-dependent term is found to be large and often larger than the static (local) one. We believe that it is important to include this nonlocality as we argued earlier [4]. Although not shown in the table for the decays of the decuplet baryons, the ratio of the nonlocal to local contribution is much larger than unity (~ 20 for case A and ~ 6 for case B).

The magnetic coupling of the ρ-meson to the nucleon is given by the isovector anomalous magnetic moment, 3.7, in the vector-dominance model, but it has been argued that its value is a factor of approximately 2 larger [14]. Our value of F_2 is nearer to the latter value than to the former for case A, but is closer to the isovector magnetic moment in case B. The isoscalar magnetic coupling, F_2^ω, for the ω meson is found to be appropriately small for both cases A and B. Tables 4 and 5 show that this ratio is independent of radius if $b = b_M$, because it depends only on $t = b_m/b$. Indeed, it is found that most ratios such as $\langle \vec{\sigma}_N \cdot \vec{Q} \rangle / \langle \vec{\sigma}_N \cdot \vec{q} \rangle$, $\langle$exchange contribution$\rangle / \langle$direct contribution$\rangle$, F_2, R_1, R_2, etc. depend only on $t = b_m/b$, and therefore are identical for all values of $b_m = b$.

---

[1] It may be more appropriate to replace m_π by the energy of the pion, E_π, since the pion is treated relativistically. See, e.g., ref. [12]

Finally, we can compare our work to that of Yu and Zhang [15]. They use a different vector-particle propagator than we do, but obtain reasonable fits to meson-nucleon coupling constants with parameters (e.g., α_s) similar to ours. They choose a definite frame of reference, namely the laboratory frame for the initial baryon and omit recoil corrections as such. Our model has been used to investigate the charge dependence of the nucleon-isospin unity meson vertices [16].

Appendix A

Defining relations for Y_d, X_{1d} to X_{4d} and Y_e, X_{1e} to X_{4e},

$$
\begin{aligned}
Y_d &= \frac{2^{1/4}\pi^{1/4}b_m^{1/2}}{3\{3+2t^2\}}\exp\left[-\frac{q^2b^2}{6}\right],\\
X_{1,d} &= 0,\\
X_{2,d} &= f_2(u),\\
X_{3,d} &= -18f_1(u),\\
X_{4,d} &= -6f_1(u)+\frac{8t^2}{3+2t^2}f_3(u),\\
Y_e &= \frac{2^{7/4}3^{3/2}\pi^{1/4}b_m^{1/2}}{(3+2t^2)^{3/2}}t\exp\left[-\frac{q^2b^2}{24}\right],\\
X_{1,e} &= \frac{1}{6t_1^3},\\
X_{2,e} &= \frac{1}{9t_1}\left(1-\frac{1}{t_1^2}\right),\\
X_{3,e} &= \frac{1}{18t_1}\left(2-\frac{5}{t_1^2}\right),\\
X_{4,e} &= \frac{1}{27}\left(-4t-\frac{10}{t_1}+\frac{5}{t_1^3}\right),
\end{aligned}
\tag{A.1}
$$

for case A and

$$
\begin{aligned}
Y_d &= \frac{2^{-11/4}\pi^{1/4}}{m_4^2b_m^{3/2}}\exp\left[-\frac{q^2b^2}{6}\right],\\
X_{1,d} &= 0,\\
X_{2,d} &= -\tfrac{1}{3},\\
X_{3,d} &= 2,\\
X_{4,d} &= \tfrac{2}{3},\\
Y_e &= -\frac{2^{5/4}3^{3/2}\pi^{1/4}t^3}{m_4^2b_m^{3/2}t_2^{3/2}}\exp\left[-\frac{q^2b^2}{24}\right]\exp\left[-\frac{3b_m^2}{2t_2}\left|\frac{\vec{Q}}{3}-\frac{\vec{q}}{2}\right|^2\right],\\
X_{1,e} &= \frac{1}{2}-\frac{3t^2}{2t_2},\\
X_{2,e} &= \frac{t^2}{t_2},
\end{aligned}
$$

$$X_{3,e} = -\frac{1}{2} + \frac{5t^2}{2t_2},$$

$$X_{4,e} = -\frac{1}{3} - \frac{5t^2}{3t_2}, \tag{A.2}$$

for case B. In these equations we use $t \equiv b_m/b$, $t_1 \equiv \sqrt{6+7t^2}/(\sqrt{2}\sqrt{3+2t^2})$ and $t_2 \equiv 6+7t^2$. The functions $f_1(u)$, $f_2(u)$, and $f_3(u)$ are

$$f_1(u) = \frac{2}{u}\int_0^\infty dx\, e^{-x^2}\sin(ux),$$

$$f_2(u) = \frac{6}{u}\int_0^\infty dx\, e^{-x^2} j_1(ux),$$

$$f_3(u) = \frac{6}{u}\int_0^\infty dx\, e^{-x^2} x^2 j_1(ux), \tag{A.3}$$

where $u = Qb_m/\sqrt{3(3+2t^2)}$. In the limit of $u \to 0$ the functions f_1, f_2 and f_3 approach unity. In these equations the same value of b is used for the initial and final baryons.

References

1. Chodos, A., et al.: Phys. Rev. **D9**, 3471 (1974)
2. Henley, E. M., Kisslinger, L. S., Miller, G. A.: Phys. Rev. **C28**, 1277 (1983)
3. Faessler, A., et al.: Phys. Lett. **112B**, 201 (1982); Nucl. Phys. **A402**, 555 (1983); Faessler, A.: Prog. Part. Nucl. Phys. **20**, 151 (1988)
4. Henley, E. M., Oka, T., Vergados, J.: Phys. Lett. **166B**, 274 (1986)
5. Henley, E. M., Oka, T., Vergados, J.: Nucl. Phys. **A476**, 589 (1988)
6. See, e.g., Henley, E. M., Su, R., Li, M., Kuyucak, S.: In: Particles and Detectors, Festschrift for Jack Steinberger (Kleinknecht, K., Lee, T. D., eds.), p. 139. New York: Springer 1986; and references therein
7. See, e.g., Green, A. M., Niskanen, J. A., Wycech, S.: Phys. Lett. **139B**, 15 (1984); Furui, S., Faessler, A., Khadhikar, S. B.: Nucl. Phys. **A424**, 495 (1984)
8. See, e.g., Weise, W.: Prog. Part. Nucl. Phys. **20**, 113 (1988)
9. Kaiser, N., Vogl, U., Weise, W., Meissner, U.-G.: Nucl. Phys. **A484**, 593 (1988)
10. See, e.g., Cooper, E. D., Jennings, B. K.: Nucl. Phys. A (submitted); and references therein
11. Dumbrajs, O., et al.: Nucl. Phys. **B216**, 277 (1983)
12. See, e.g., Henley, E. M., Ruderman, M. A.: Phys. Rev. **90**, 719 (1953); Ho, H. W., Alberg, M. A., Henley, E. M.: Phys. Rev. **C12**, 217 (1975)
13. See, e.g., Kohno, M., Weise, W.: Phys. Lett. **152B**, 303 (1985); Nucl. Phys. **A454**, 429 (1986)
14. See, e.g., Brown, G. E.: Nucl. Phys. **A446**, 3c (1985)
15. Yu, Y.-W., Zhang, Z.-Y.: Nucl. Phys. **A426**, 557 (1984); Yu, Y.-W.: Nucl. Phys. **A455**, 737 (1986)
16. Henley, E. M., Zhang, Z.-Y.: Nucl. Phys. **A472**, 759 (1987)
17. Particle Data Group: Phys. Lett. **204B**, 1 (1988)

Received August 1, 1989; revised November 14, 1989; accepted for publication May 15, 1990